

High-performance 30-period quantum-dot infrared photodetector

Shu-Ting Chou, Shih-Yen Lin, Ru-Shang Hsiao, Jim-Yong Chi, Jyh-Shyang Wang, Meng-Chyi Wu, and Jenn-Fang Chen

Citation: *Journal of Vacuum Science & Technology B* **23**, 1129 (2005); doi: 10.1116/1.1900730

View online: <http://dx.doi.org/10.1116/1.1900730>

View Table of Contents: <http://scitation.aip.org/content/avs/journal/jvstb/23/3?ver=pdfcov>

Published by the AVS: Science & Technology of Materials, Interfaces, and Processing

Articles you may be interested in

[Tuning the photoresponse of quantum dot infrared photodetectors across the 8 – 12 \$\mu\$ m atmospheric window via rapid thermal annealing](#)

Appl. Phys. Lett. **91**, 143502 (2007); 10.1063/1.2794014

[High-performance InAs quantum-dot infrared photodetectors grown on InP substrate operating at room temperature](#)

Appl. Phys. Lett. **90**, 131112 (2007); 10.1063/1.2719160

[Multispectral operation of self-assembled InGaAs quantum-dot infrared photodetectors](#)

Appl. Phys. Lett. **85**, 4154 (2004); 10.1063/1.1810208

[High detectivity InGaAs/InGaP quantum-dot infrared photodetectors grown by low pressure metalorganic chemical vapor deposition](#)

Appl. Phys. Lett. **84**, 2166 (2004); 10.1063/1.1688982

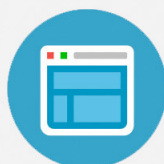
[Influence of rapid thermal annealing on a 30 stack InAs/GaAs quantum dot infrared photodetector](#)

J. Appl. Phys. **94**, 5283 (2003); 10.1063/1.1609634



Re-register for Table of Content Alerts

Create a profile.



Sign up today!



High-performance 30-period quantum-dot infrared photodetector

Shu-Ting Chou

Department of Electrical Engineering, National Tsing Hua University, Hsinchu, Taiwan

Shih-Yen Lin^{a)}

Nanophotonics Center, Opto-Electronics and Systems Laboratories, Industrial Technology Research Institute, Hsinchu, Taiwan

Ru-Shang Hsiao

Department of Electrophysics, National Chiao Tung University, Hsinchu, Taiwan

Jim-Yong Chi and Jyh-Shyang Wang

Nanophotonics Center, Opto-Electronics and Systems Laboratories, Industrial Technology Research Institute, Hsinchu, Taiwan

Meng-Chyi Wu

Department of Electrical Engineering, National Tsing Hua University, Hsinchu, Taiwan

Jenn-Fang Chen

Department of Electrophysics, National Chiao Tung University, Hsinchu, Taiwan

(Received 27 October 2004; accepted 7 March 2005; published 7 June 2005)

In this article, quantum-dot infrared photodetectors (QDIPs) with 10- and 30-period InAs/GaAs quantum-dot structures are investigated. High responsivity of 2.37 A/W and detectivity of $2.48 \times 10^{10} \text{ cm Hz}^{1/2}/\text{W}$ for 30-period QDIPs under 10 K are observed at -2.7 and 1.2 V, respectively. Almost symmetric photocurrents and dark currents under positive and negative biases are observed for both devices, which indicate a minor influence of the wetting layer on the performance of QDIPs. Lower dark current and increased photocurrent for the 30-period QDIPs would predict a better performance for devices with over a 30-period QD structure. © 2005 American Vacuum Society. [DOI: 10.1116/1.1900730]

With self-assembled InAs/GaAs quantum dots (QDs) as the absorption medium, QD infrared photodetectors (QDIPs) have revealed its potential in the application of infrared (IR) detection.¹⁻¹¹ Compared with conventional quantum-well infrared photodetectors, normal-incident absorption, wider detection window, and higher-temperature operation are reported.¹⁻⁷ However, the influences of sample structures on the device performances are not optimized yet. In this article, the influence of InAs/GaAs QD layer number on the performances of QDIPs is investigated. Compared with a 10-period QDIP, higher responsivity and detectivity are observed for a 30-period QDIP. Also observed is the symmetric photo- and dark currents for both devices, which implies the minor influence of a wetting layer on the performances of the QDIPs. A discontinuity observed in the dark current measurement for a 30-period QDIP is attributed to the occurrence of sequential resonant tunneling under appropriate voltage.¹²

The InAs/GaAs QD samples are prepared by Riber Epineat solid-source molecular-beam epitaxy on semi-insulating GaAs substrates. 10- or 30-period 2.63 monolayer (ML) InAs/30 nm GaAs QDIP samples, referred to as Devices A or B are sandwiched between 0.5 and 1 μm thick GaAs contact layers with $n=1 \times 10^{18} \text{ cm}^{-3}$. The InAs QD region is n -type doped to $1 \times 10^{18} \text{ cm}^{-3}$. The growth temperature for the InAs QDs is 495 °C, while a higher growth temperature, 600 °C, is adopted for the GaAs barrier layers.

After mesa formation and metal evaporation, $100 \times 100 \mu\text{m}^2$ devices are fabricated. The device structure is shown in Fig. 1. and the insert in the figure shows the atomic force microscopy (AFM) image of the InAs QDs grown under the same growth condition. Uniform QD distribution is observed from the AFM image. According to the AFM measurements, the QD density is $\sim 7 \times 10^{10} \text{ cm}^{-2}$. The $1 \times 10^{18} \text{ cm}^{-3}$ doping density at the InAs QD region would therefore correspond to a Si donor at each QD on average. The measurement of spectral responses is performed under an edge-coupling scheme.⁴⁻⁶ For this purpose, the devices are 45° polished at one side of the sample. The measurement system for spectral responses consists of a Spectral One Fourier transformation spectroscopy coupling with ARC cryo-

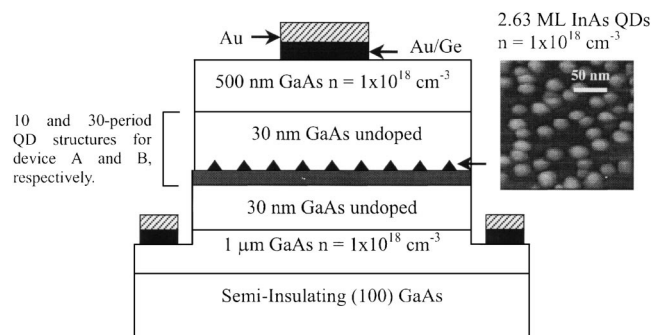


FIG. 1. Device structures of Devices A and B. The inset shows the AFM image of the InAs QDs grown under the same growth condition.

^{a)}Electronic mail: linshihyen@itri.org.tw

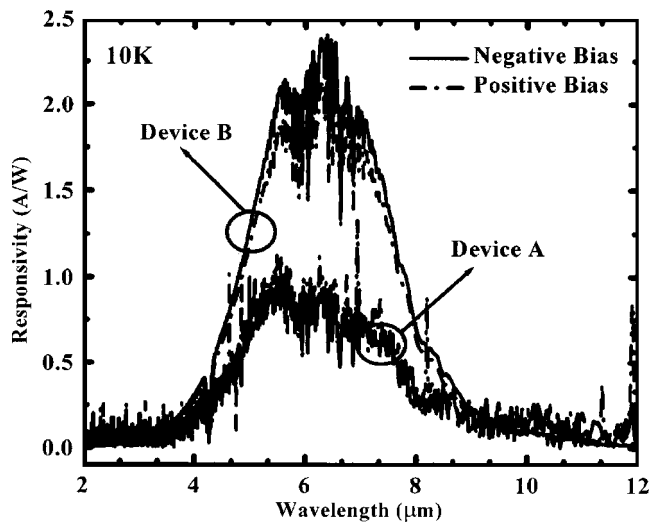


Fig. 2. 10 K spectral responses of Devices A and B at +0.7 and +2.7 V, respectively.

genics and a MODEL SR570 current preamplifier. Temperature-dependent dark current-voltage characteristics are measured with a Keithley 236 source measure unit at the same ARC cryogenics.

The spectral responses measured at 10 K with different applied voltages are shown in Fig. 2. Higher peak responsivity 2.37 A/W at -2.7 V is observed for Device B while Device A shows a peak of 0.98 A/W at -0.7 V. The photocurrent for Device B is three times higher than that of Device A for the same electrical field. This increase indicated a non-saturated photocurrent up to a 30-period QD structure. Higher responsivity with more than a 30-period QD structure is expected. Another phenomenon observed in Fig. 2 is the symmetric photocurrents for both devices under positive and negative biases. According to a previous report,¹⁵ the spectral response of a InAs/GaAs QDIP consists of several transition mechanisms involving QD confinement states to wetting layer photoexcitation. The wetting layer-to-continuum transition is not observed either under an edge-coupling scheme or normal-incident condition. And, due to the fact that the multistacked QD structure is always adopted for QDIPs, the incident IR light has to go through multi-QD and wetting layer regions either under normal-incident or edge-coupling conditions. Therefore, the phenomena of symmetric photocurrents are attributed to the minor influences of the wetting layer and the three-dimensional character of the InAs QDs on the performance of the QDIPs.

The spectral responses of Device B under 10, 50, and 100 K at an applied voltage of 0.5 V are shown in Fig. 3. Increasing spectral responses with increasing temperature is observed, where a more pronounced increase in the wavelength range of 3–6 μm is observed. This phenomenon is attributed to the depopulation of electrons at the excited states with increasing temperature, such that the ground-to-excited state transition is increased.⁴ The detectivity D^* is determined following the equation that detectivity $D^* = R(AB)^{1/2}/i_n$, where R , A , i_n , and B are the peak responsivity,

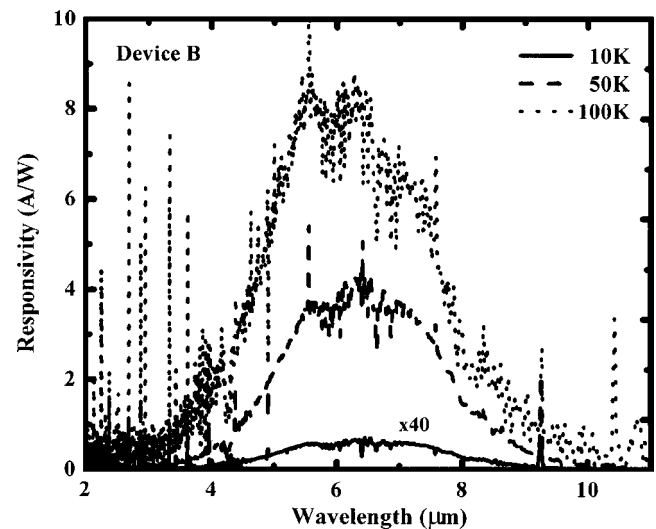


Fig. 3. Spectral response of Device B under 10, 50, and 100 K at applied voltage 0.5 V.

ity, device area, noise current, and measurement bandwidth, respectively. The noise current, i_n , could be derived through the relation $i_n^2 = 4egI_dB$, where I_d is the current under the dark environment and g is the gain assumed to be 1.^{3–6} The 6.2 μm peak detectivities for Device B at 0.5 V under 10, 50, and 100 K are 6.25×10^8 , 3.82×10^7 , and 2.66×10^7 $\text{cm}^2 \text{Hz}^{1/2}/\text{W}$, respectively. Although high responsivity of 8 A/W is observed with increasing temperature up to 100 K, the peak detectivities at 6.2 μm decrease due to the more rapid increase of dark current with increasing temperature compared with the case for photocurrent.

The dark current densities for Devices A and B under 10 K are shown in Fig. 4. The lower dark current for Device B is attributed to the increase of QD period such that the total barrier thickness is increased. Also shown in Fig. 4 is the abrupt dark current increase for Device B at ~ 1.5 and -1 V, respectively, which is attributed to the sequential reso-

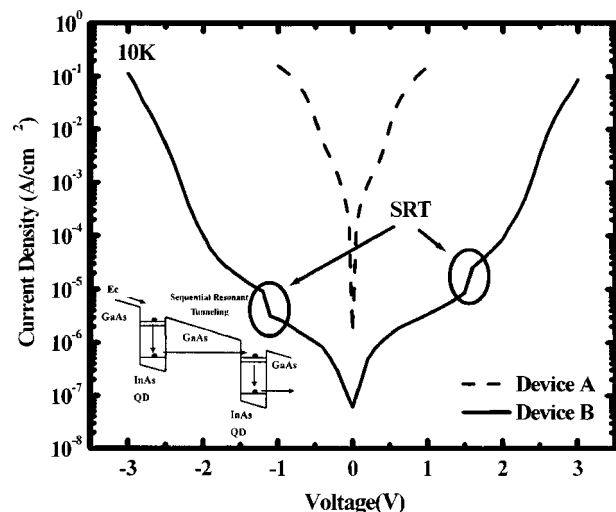


Fig. 4. Dark current density of Devices A and B under 10 K. The inset shows the schematic diagram for the phenomenon of SRT.

nant tunneling (SRT) at an appropriate voltage as shown in the inset of Fig. 4.¹² Since the dominant dark current component for a temperature higher than 60 K is the thermionic emission current,^{10,11} the activation energies under different biases can be derived through the curve fitting for the dark currents with the equation $I_D \sim T^2 e^{-E_a/kT}$, where T is temperature and E_a is the activation energy which equals $(\Delta E_c - E_F)$.⁶ ΔE_c is the conduction-band discontinuity and E_F is the Fermi level. The derived zero-bias activation energies are 25 and 112 meV for Devices A and B, respectively. Symmetric activation energies under different polarities of applied voltage are consistent with the symmetric photocurrent. Higher activation energy at zero-applied bias for Device B would indicate a lower dark current with an increasing QD layer number. Due to the higher photocurrent and lower dark current, high $6.2 \mu\text{m}$ detectivity of $2.48 \times 10^{10} \text{ cm Hz}^{1/2}/\text{W}$ for Device B at 10 K with responsivity $42.9 \text{ mA}/\text{W}$ at 1.2 V is observed. Compared with the peak detectivity $1.08 \times 10^9 \text{ cm Hz}^{1/2}/\text{W}$ with responsivity $16.4 \text{ mA}/\text{W}$ for Device A, Device B has ~ 20 times higher peak detectivity. A higher detectivity of Device B results in a higher background-limited performance temperature of 60 K compared with 30 K for Device A.

In conclusion, symmetric photocurrents and dark currents under positive and negative biases are observed for both devices, which indicate a minor influence of the wetting layer and the three-dimensional character of the InAs QDs on the performance of QDIPs. And due to the increase of dark currents usually being more pronounced than photocurrents, the

phenomenon would result in different applied voltages for peak detectivity and peak responsivity to occur. Therefore, for a 30-period QDIP under 10 K, peak responsivity of $2.37 \text{ A}/\text{W}$ and detectivity of $2.48 \times 10^{10} \text{ cm Hz}^{1/2}/\text{W}$ are observed at -2.7 and 1.2 V , respectively. Lower dark current and nonsaturated photocurrent for the 30-period QDIP would indicate that better performance could be obtained for devices with a layer number over 30. A discontinuity observed in the dark current measurement at ~ 1.5 and -1 V for the 30-period QDIP is attributed to the occurrence of SRT.

¹J. Phillips, K. Kamath, and P. Bhattacharya, *Appl. Phys. Lett.* **72**, 2020 (1998).

²D. Pan, E. Towe, and S. Kennerly *Appl. Phys. Lett.* **73**, 1937 (1998).

³S. Chakrabarti, A. D. Stiff-Roberts, P. Bhattacharya, S. Gunapala, S. Bandara, S. B. Rafol, and S. W. Kennerly, *IEEE Photonics Technol. Lett.* **16**, 1361 (2004).

⁴S.-Y. Lin, Y.-R. Tsai, and S.-C. Lee, *Jpn. J. Appl. Phys., Part 2* **40**, L1290 (2001).

⁵S.-Y. Lin, Y.-R. Tsai, and S.-C. Lee, *Appl. Phys. Lett.* **83**, 752 (2003).

⁶S.-Y. Lin, Y.-R. Tsai, and S.-C. Lee, *Appl. Phys. Lett.* **78**, 2784 (2001).

⁷D. Pan, E. Towe, and S. Kennerly, *Appl. Phys. Lett.* **75**, 2719 (1999).

⁸Z. Chen, O. Baklenov, E. T. Kim, I. Mukhametzhano, J. Tie, A. Madhukar, Z. Ye, and J. C. Campbell, *J. Appl. Phys.* **89**, 4558 (2001).

⁹Z. Chen, E. T. Kim, and A. Madhukar, *Appl. Phys. Lett.* **80**, 2490 (2002).

¹⁰A. D. Stiff-Roberts, X. H. Su, S. Chakrabarti, and P. Bhattacharya, *IEEE Photonics Technol. Lett.* **16**, 867 (2004).

¹¹J. Y. Duboz, H. C. Liu, Z. R. Wasilewski, M. Byloss, and R. Dudek, *J. Appl. Phys.* **93**, 1320 (2003).

¹²K. K. Choi, *The Physics of Quantum Well Infrared Photodetectors* (World Scientific, Singapore, 1997), Chap. 9.

¹³H. C. Liu, M. Gao, J. McCaffrey, Z. R. Wasilewski, and S. Fafard, *Appl. Phys. Lett.* **78**, 79 (2001).